

File SFPHYS4.DOC contains the following bookmarks. Select the topic you are trying to find from the list and double click the highlighted text.

[BoundaryConditions](#)
[CalculationOfFields](#)
[CorrectionsIn1987manual](#)
[NumericalMethods](#)
[DirectMethod](#)
[SORmethod](#)
[VectorPotentialOnMeshPoint](#)

Physics discussions in other files

SFPHYS1.DOC	Theory of electrostatics and magnetostatics
SFPHYS2.DOC	Properties of static magnetic and electric fields
SFPHYS3.DOC	Boundary conditions and symmetries
SFPHYS5.DOC	RF cavity theory

File SFPHYS4.DOC Table of Contents

XXIII. Numerical Methods in Poisson and Pandira	579
A. Mesh formulation	579
B. Calculation of the vector potential at a mesh point	580
C. Application of boundary conditions	594
D. Calculation of fields	596
E. Computer algorithm using the SOR method	597
F. Computer algorithm using the direct method	598

XXIII. Numerical Methods in Poisson and Pandira

This section is based upon the treatment in Part B, Chapter 13.6 by John L. Warren in the 1987 publication Reference Manual for the POISSON/SUPERFISH Group of Codes, LA-UR-87-126. The original chapter was titled “Numerical Methods Used in POISSON and PANDIRA.” We reproduce it here in essentially its original form as reference material to the physics in the Poisson Superfish codes. The equation sequence numbers are the same as in the original. We have corrected a few typographical errors in the original, including the following:

- Equation XXIII-46 had two extra left parentheses, one each in each of the numerators of the last two terms.
- The left-hand side of Equation XXIII-62 was z_1^* . The correct term is z_2^* .
- Equation XXIII-64 included the term β_0 where it should have used β_1 .
- On the first line of Equation XXIII-67, the term A_2 should be A_6 .

The customary way to solve the magnetostatic problem would be to map the interior region with a mesh and then solve for the vector potential at these mesh points using a discretized form of Poisson’s equation and the necessary boundary conditions. The procedure used in this program does not directly solve Poisson’s equation; rather, it solves a form of Ampere’s Law over a closed region made up of triangular plates. The procedure is iterative using either a successive over-relaxation (SOR) algorithm (as in Poisson) or a direct matrix-inversion method (as in Pandira) combined with an iterative correction scheme for the reluctivity function. The solution is the vector potential at each mesh point (i.e., the vertices of the triangles). The discussion is divided into the following sections:

- Mesh formulation,
- Calculation of the vector potential at a mesh point,
- Application of boundary conditions,
- Calculation of fields,
- Computer algorithm using the SOR method, and
- Computer algorithm using the direct method.

A. Mesh formulation

The program Automesh generates an irregular triangular mesh over the region, within the boundaries conforming to the following rules:

- The triangulation forms a regular topology, that is, an array of equilateral triangles in which six triangles meet at every interior mesh point,
- All triangles within an interior region are characterized by a common set of attributes such as current density, permeability, etc., and

- Any triangle along an external boundary or a boundary of a closed interior region will have two of its vertices lying on these boundary-defining lines. These boundaries will then be described by piecewise linear segments which are the sides of the interpolating triangles.

Since any polygonal region can be triangulated, the method can be applied to regions of any shape and will produce a mesh in which boundaries and interfaces lie entirely on mesh lines. In those areas where the gradient of the vector potential is expected to be large the triangles should be made more dense.

B. Calculation of the vector potential at a mesh point

The procedure in programs Poisson and Pandira solves for the vector potential $\mathbf{A}(\mathbf{r})$ at each mesh point using a relationship derived from Ampere's Law,

$$\oint_C \mathbf{H}(\mathbf{r}) \cdot d\mathbf{l} = \int_S \mathbf{J}(\mathbf{r}) \cdot \hat{\mathbf{n}} da, \quad (\text{XXIII-1})$$

where $\mathbf{H}(\mathbf{r})$ is the magnetic field, $\mathbf{J}(\mathbf{r})$ is the current density, \mathbf{r} is a vector written as follows in terms of unit vectors along the coordinate axes: $\mathbf{r} = r_x \hat{\mathbf{e}}_x + r_y \hat{\mathbf{e}}_y + r_z \hat{\mathbf{e}}_z$, $\hat{\mathbf{n}}$ is a unit vector normal to the surface S , and C is the contour of the line integral enclosing the surface S . The solution is iterative in nature in that the calculated value of the vector potential at a mesh point is a function of previous estimates and arbitrary initializations. Over each triangular area, we make the approximations that

- the vector potential is linear,
- the reluctivity is constant, and
- the current density is constant.

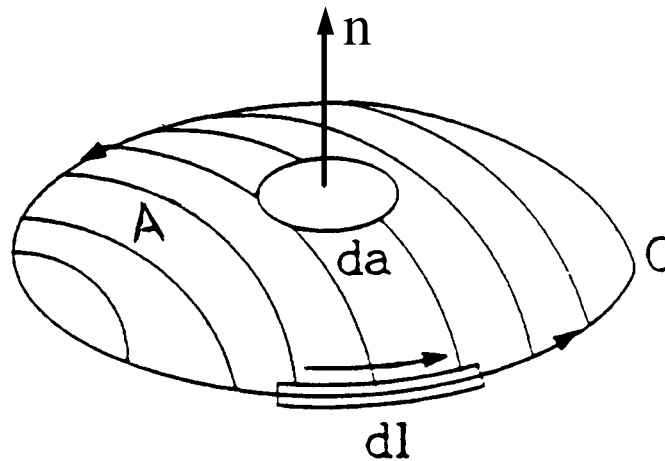


Figure XXIII-1. Surface and contour elements in Equation XXIII-1.

Since Equation XXIII-1 must be expressed in terms of the vector potential $\mathbf{A}(\mathbf{r})$, the first step is to express the magnetic field $\mathbf{H}(\mathbf{r})$ in terms of the reluctivity $\gamma(|\mathbf{B}(\mathbf{r})|)$ and the magnetic induction $\mathbf{B}(\mathbf{r})$. This relationship is

$$\gamma(|\mathbf{B}(\mathbf{r})|)\mathbf{B}(\mathbf{r}) = \mu_0\mathbf{H}(\mathbf{r}). \quad (\text{XXIII-2})$$

By substituting for $\mathbf{H}(\mathbf{r})$ in Equation XXIII-1, Ampere's Law becomes

$$\oint_C \gamma(|\mathbf{B}(\mathbf{r})|)\mathbf{B}(\mathbf{r}) \cdot d\mathbf{l} = \mu_0 \int_S \mathbf{J}(\mathbf{r}) \cdot \hat{\mathbf{n}} da. \quad (\text{XXIII-3})$$

The final step is to use the fact that the magnetic induction $\mathbf{B}(\mathbf{r})$ is the curl of the vector potential, namely,

$$\mathbf{B}(\mathbf{r}) = \nabla \times \mathbf{A}(\mathbf{r}). \quad (\text{XXIII-4})$$

Substituting this equation into Equation XXIII-3 gives the required form

$$\oint_C \gamma(|\mathbf{B}(\mathbf{r})|)\nabla \times \mathbf{A}(\mathbf{r}) \cdot d\mathbf{l} = \mu_0 \int_S \mathbf{J}(\mathbf{r}) \cdot \hat{\mathbf{n}} da. \quad (\text{XXIII-5})$$

Next, the curl is expanded in terms of its components, giving

$$\nabla \times \mathbf{A}(\mathbf{r}) = \left(\frac{\partial A_z}{\partial y} - \frac{\partial A_y}{\partial z} \right) \hat{\mathbf{e}}_x + \left(\frac{\partial A_x}{\partial z} - \frac{\partial A_z}{\partial x} \right) \hat{\mathbf{e}}_y + \left(\frac{\partial A_y}{\partial x} - \frac{\partial A_x}{\partial y} \right) \hat{\mathbf{e}}_z. \quad (\text{XXIII-6})$$

By definition in Poisson and Pandira, the induction $\mathbf{B}(\mathbf{r})$ is a two-dimensional vector lying in the x-y plane. The vector potential $\mathbf{A}(\mathbf{r})$ can then be chosen normal to this plane with only the A_z component being nonzero,

$$A_x = A_y = 0. \quad (\text{XXIII-7})$$

A necessary condition to be satisfied for Poisson's equation, in addition to Ampere's Law, is that of the Coulomb gauge choice,

$$\nabla \cdot \mathbf{A}(\mathbf{r}) = 0, \quad (\text{XXIII-8})$$

which can be expanded in the following form,

$$\frac{\partial A_x}{\partial x} + \frac{\partial A_y}{\partial y} + \frac{\partial A_z}{\partial z} = 0. \quad (\text{XXIII-9})$$

Since Equation XXIII-7 implies that

$$\frac{\partial A_x}{\partial x} = \frac{\partial A_y}{\partial y} = 0, \quad (\text{XXIII-10})$$

the only remaining condition from Equation XXIII-9 is

$$\frac{\partial A_z}{\partial z} = 0. \quad (\text{XXIII-11})$$

This equation is equivalent to the statement that the vector potential A_z is not a function of z . By making the position vector \mathbf{r} a two-dimensional vector in the x - y plane, the Coulomb gauge condition has been satisfied. Henceforth, it will be understood that

$$\mathbf{r} = r_x \hat{\mathbf{e}}_x + r_y \hat{\mathbf{e}}_y. \quad (\text{XXIII-12})$$

It follows that

$$\mathbf{B} = \nabla \times \mathbf{A}(\mathbf{r}) = \frac{\partial A_z}{\partial y} \hat{\mathbf{e}}_x - \frac{\partial A_z}{\partial x} \hat{\mathbf{e}}_y, \quad (\text{XXIII-13})$$

and Equation XXIII-5 becomes

$$\oint_C \gamma(|\mathbf{B}(\mathbf{r})|) \left[\frac{\partial A_z}{\partial y} \hat{\mathbf{e}}_x - \frac{\partial A_z}{\partial x} \hat{\mathbf{e}}_y \right] \cdot d\mathbf{l} = \mu_0 \int_S \mathbf{J}(\mathbf{r}) \cdot \hat{\mathbf{n}} da. \quad (\text{XXIII-14})$$

This rest of section will develop the equations in Cartesian coordinates; the theory in cylindrical coordinates is similar. Before continuing with this derivation, a brief discussion of the complex notation may be helpful. A two-dimensional vector

$$\mathbf{a} = a_x \hat{\mathbf{e}}_x + a_y \hat{\mathbf{e}}_y, \quad (\text{XXIII-15})$$

can be represented as a complex number

$$a = a_x + i a_y. \quad (\text{XXIII-16})$$

The complex conjugate of a is defined by the relation

$$a^* = a_x - i a_y. \quad (\text{XXIII-17})$$

Given two vectors

$$\mathbf{a} = a_x \hat{\mathbf{e}}_x + a_y \hat{\mathbf{e}}_y, \quad (\text{XXIII-18})$$

$$\mathbf{b} = b_x \hat{\mathbf{e}}_x + b_y \hat{\mathbf{e}}_y, \quad (\text{XXIII-19})$$

and their complex representation

$$a = a_x + i a_y, \quad (\text{XXIII-20})$$

$$b = b_x + i b_y, \quad (\text{XXIII-21})$$

then the product $a^* b$ can be written as

$$a^* b = (a_x - i a_y)(b_x + i b_y) = a_x b_x + a_y b_y + i(a_x b_y - a_y b_x), \quad (\text{XXIII-22})$$

and contains both the scalar and vector products of the vectors, namely,

$$\mathbf{a} \cdot \mathbf{b} = a_x b_x + a_y b_y, \quad (\text{XXIII-23})$$

$$\mathbf{a} \times \mathbf{b} = (a_x b_y - a_y b_x) \hat{\mathbf{e}}_z. \quad (\text{XXIII-24})$$

Hence we can write

$$\mathbf{a}^* \mathbf{b} = \mathbf{a} \cdot \mathbf{b} + i \hat{\mathbf{e}}_z \cdot (\mathbf{a} \times \mathbf{b}), \quad (\text{XXIII-25})$$

and it follows that

$$\mathbf{a} \cdot \mathbf{b} = \text{Re}(\mathbf{a}^* \mathbf{b}). \quad (\text{XXIII-26})$$

The above equation can be used to get the integrand on the left-hand side of Equation XXIII-14 into a tractable form. Corresponding to the relationship between the vector $\mathbf{B}(\mathbf{r})$ and the vector potential,

$$\mathbf{B}(\mathbf{r}) = \frac{\partial A_z}{\partial y} \hat{\mathbf{e}}_x - \frac{\partial A_z}{\partial x} \hat{\mathbf{e}}_y, \quad (\text{XXIII-27})$$

one can define a complex function

$$B(x, y) = \frac{\partial A_z}{\partial y} + i \left(-\frac{\partial A_z}{\partial x} \right) = B_x + i B_y, \quad (\text{XXIII-28})$$

and its complex conjugate

$$B^*(x, y) = \frac{\partial A_z}{\partial y} - i \frac{\partial A_z}{\partial x} = B_x - i B_y, \quad (\text{XXIII-29})$$

The vector $d\mathbf{l}$ will not be represented as a sum of its components but rather as a complex number dl . The logic for this representation will be seen later in the analysis. The integrand, excluding the $\gamma(|\mathbf{B}(\mathbf{r})|)$ term, in this complex notation is

$$\mathbf{B}(\mathbf{r}) \cdot d\mathbf{l} = \text{Re}(B^* dl) = \text{Re} \left[\left(\frac{\partial A_z}{\partial y} + i \frac{\partial A_z}{\partial x} \right) dl \right]. \quad (\text{XXIII-30})$$

The potential A_z can be viewed as a scalar function of the complex number z , namely,

$$A_z(x, y) = A_z(z) = A_z(x + i y). \quad (\text{XXIII-31})$$

It is also useful to think of A_z as a function of both z and z^* since

$$x = \frac{1}{2}(z + z^*) \quad \text{and} \quad y = \frac{1}{2i}(z^* - z). \quad (\text{XXIII-32})$$

Now evaluate the partial derivatives $\partial A_z(z, z^*)/\partial x$ and $\partial A_z(z, z^*)/\partial y$. It is easy to see that

$$\frac{\partial A_z(z, z^*)}{\partial x} = \frac{\partial A_z(z, z^*)}{\partial z} \frac{\partial z}{\partial x} + \frac{\partial A_z(z, z^*)}{\partial z^*} \frac{\partial z^*}{\partial x}, \quad (\text{XXIII-33})$$

and

$$\frac{\partial A_z(z, z^*)}{\partial y} = \frac{\partial A_z(z, z^*)}{\partial z} \frac{\partial z}{\partial y} + \frac{\partial A_z(z, z^*)}{\partial z^*} \frac{\partial z^*}{\partial y}. \quad (\text{XXIII-34})$$

Because of the relations

$$\frac{\partial z}{\partial x} = 1, \quad \frac{\partial z^*}{\partial x} = 1, \quad (\text{XXIII-35})$$

$$\frac{\partial z}{\partial y} = i, \quad \frac{\partial z^*}{\partial y} = -i, \quad (\text{XXIII-36})$$

it follows that the partial derivatives can be expressed as

$$\frac{\partial A_z(z, z^*)}{\partial x} = \left(\frac{\partial}{\partial z} + \frac{\partial}{\partial z^*} \right) A_z(z, z^*), \quad (\text{XXIII-37})$$

and

$$\frac{\partial A_z(z, z^*)}{\partial y} = i \left(\frac{\partial}{\partial z} - \frac{\partial}{\partial z^*} \right) A_z(z, z^*). \quad (\text{XXIII-38})$$

Substituting these relations into Equation XXIII-29 gives

$$B^*(x, y) = i \left[\frac{\partial}{\partial z} + \frac{\partial}{\partial z^*} - i^2 \left(\frac{\partial}{\partial z} - \frac{\partial}{\partial z^*} \right) \right] A_z(z, z^*)$$

or

$$B^*(x, y) = 2i \frac{\partial A_z(z, z^*)}{\partial z}. \quad (\text{XXIII-39})$$

Equation XXIII-30, with this new notation, becomes

$$\mathbf{B}(\mathbf{r}) \cdot d\mathbf{l} = \text{Re} \left[2i \frac{\partial A_z(z, z^*)}{\partial z} d\mathbf{l} \right]. \quad (\text{XXIII-40})$$

A few words about the intended numerical scheme are appropriate at this point. The vector potential at each mesh point, including the boundary points, is calculated as a function of the following attributes of the six surrounding triangles:

- The magnitude and position of the vector potentials at each of the surrounding six mesh points,
- The area of each of these triangles,
- The current density of each of these triangles, and
- The reluctivity of each of these triangles.

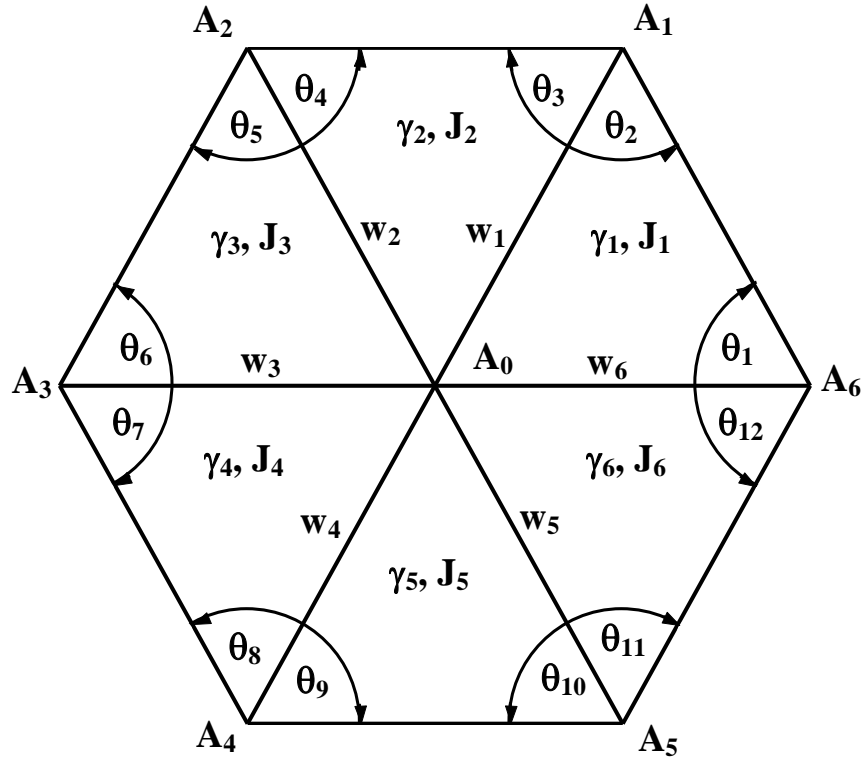


Figure XXIII-2. Physical parameters in the mesh geometry. Mesh points are numbered 0 through 6, triangles and shared triangle legs are numbered 1 through 6. The term A_i is the vector potential at mesh point i . The reluctivity in triangle i is γ_i and the current density is J_i . The w_i terms are coupling parameters.

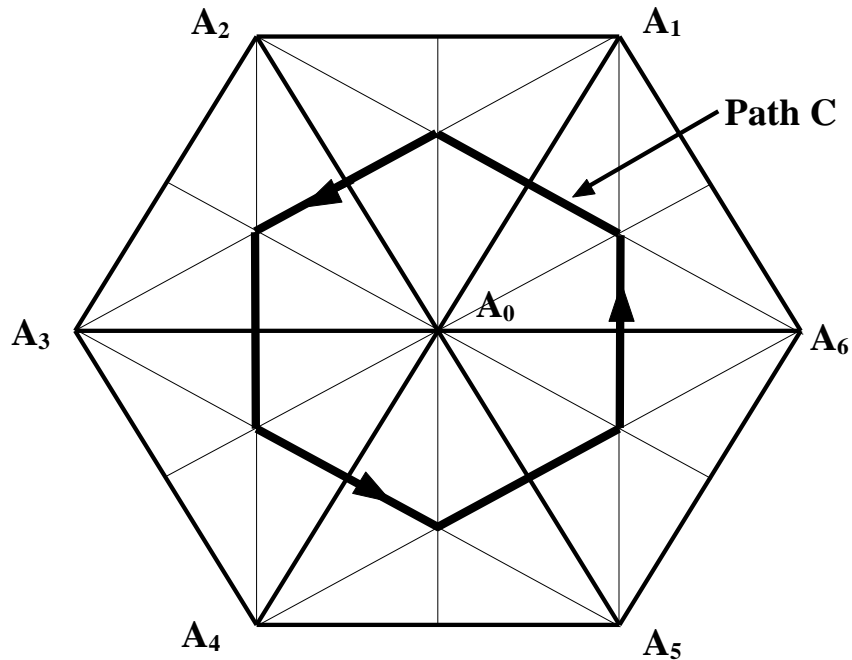


Figure XXIII-3. Path of contour integration for Ampere's Law.

The geometry used to calculate the vector potential A_0 is shown in Figure XXIII-2. For convenience, we adopt the following notation:

$$A_i \equiv A_z(z_i, z_i^*) \quad \text{and} \quad J_i \equiv J_z(z_i, z_i^*).$$

Ampere's Law is now applied to a contour around the point $i = 0$. The contour is not on the circumference of this hexagon, but rather on a dodecagon whose circumference passes through the midpoints of each side shared by two triangles and the respective centroids of each triangle. The path is shown in Figure XXIII-3.

The procedure for evaluating the integrals will be developed for one of the triangles, which is shown in Figure XXIII-4. We arbitrarily designate this triangle as "triangle 2", and then generalize for all six triangles forming the dodecagon in Figure XXIII-3. In the complex notation, Ampere's equation for the area A within the bold contour in Figure XXIII-4 is

$$\oint_C \gamma_2(|\mathbf{B}(\mathbf{r})|) \operatorname{Re} \left[2i \frac{\partial A}{\partial z} dl \right] = \mu_0 J_2 \frac{a_2}{3}. \quad (\text{XXIII-41})$$

where C is the path (p_0, p_1, p_2, p_3, p_0), a_2 is the area of triangle 2, J_2 is the normal component of current density in triangle 2, γ_2 is the reluctivity for triangle 2, and μ_0 is $4\pi \times 10^{-7}$ T-m/A.

To evaluate the left-hand side of Equation XXIII-41, a functional relationship of the vector potential over the triangle must be developed. The assumption of the solver program is that the vector potential varies linearly over any triangle in the mesh. [Note: after the solution has been obtained on all the mesh points, the [field interpolator](#) uses a more sophisticated method for computing the fields at points inside of triangles.] Using the three-point form for the equation of a plane, an expression for the vector potential at any point can be developed. The positions of the three vertices and their respective vector potentials determine the coefficients of the expression. The three-point form can be written as the determinant,

$$\begin{vmatrix} z - z_0 & z^* - z_0^* & A - A_0 \\ z_1 - z_0 & z_1^* - z_0^* & A_1 - A_0 \\ z_2 - z_0 & z_2^* - z_0^* & A_2 - A_0 \end{vmatrix} = 0. \quad (\text{XXIII-42})$$

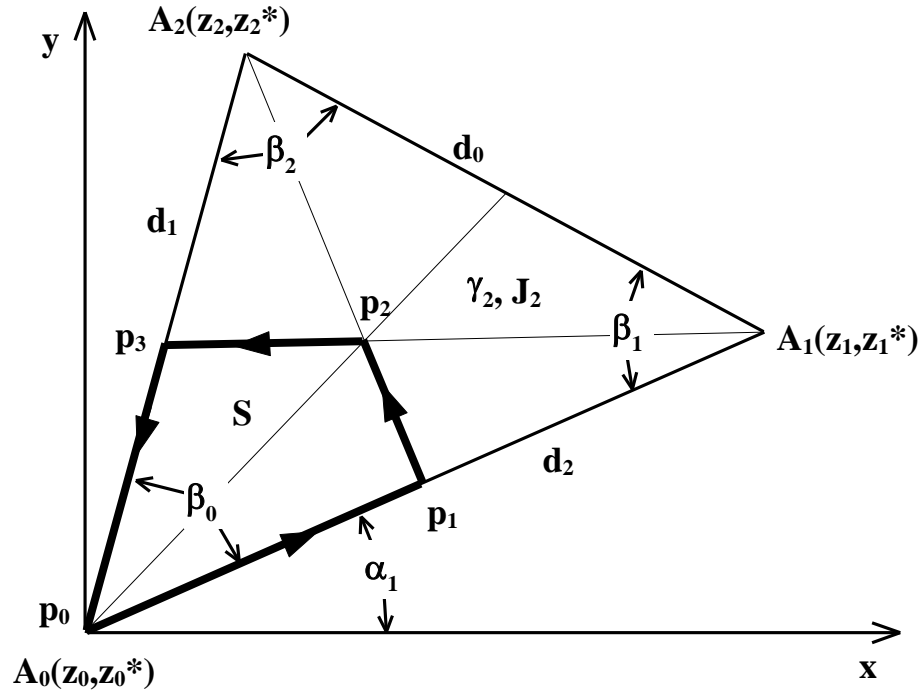


Figure XXIII-4. Contour integration details.

The contour integration over the dodecagon shown in Figure XXIII-3 can be broken into an integration over six quadrangles. The heavy line shows the path around surface S .

Figure XXIII-5 shows the plane in function space. We now expand this determinant and solve for A . Introduce the notation

$$\Delta A_1 = A_1 - A_0, \quad (\text{XXIII-43})$$

$$\Delta A_2 = A_2 - A_0. \quad (\text{XXIII-44})$$

Expanding the determinant results in the equation

$$\begin{aligned} & (z - z_0)(z_1^* - z_0^*)\Delta A_2 + (z_2 - z_0)(z^* - z_0^*)\Delta A_1 \\ & + (z_1 - z_0)(z_2^* - z_0^*)(A - A_0) - (z_2 - z_0)(z_1^* - z_0^*)(A - A_0) \\ & - (z - z_0)(z_2^* - z_0^*)\Delta A_1 - (z_1 - z_0)(z^* - z_0^*)\Delta A_2 = 0, \end{aligned} \quad (\text{XXIII-45})$$

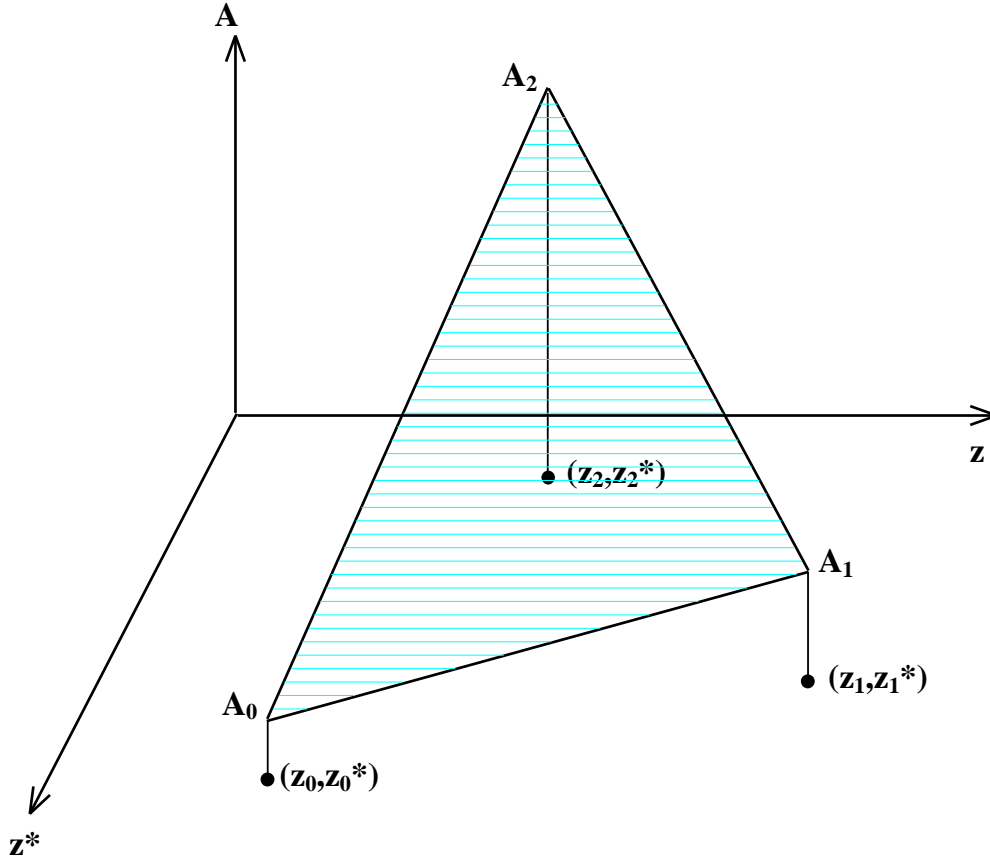


Figure XXIII-5. The vector potential is a linear function over a triangle.
The functional dependence of $A(z, z^*)$ is completely determined by the values of A at the corners of the triangle.

which can be solved for A , giving

$$A = A_0 + \frac{\Delta A_1 [(z - z_0)(z_2^* - z_0^*) - (z_2 - z_0)(z^* - z_0^*)]}{(z_1 - z_0)(z_2^* - z_0^*) - (z_2 - z_0)(z_1^* - z_0^*)} + \frac{\Delta A_2 [(z_1 - z_0)(z^* - z_0^*) - (z - z_0)(z_1^* - z_0^*)]}{(z_1 - z_0)(z_2^* - z_0^*) - (z_2 - z_0)(z_1^* - z_0^*)}. \quad (\text{XXIII-46})$$

Taking the origin at the coordinates (z_0, z_0^*) reduces Equation XXIII-46 to

$$A = A_0 + \frac{\Delta A_1 z_2^* - \Delta A_2 z_1^*}{z_1 z_2^* - z_2 z_1^*} z + \frac{\Delta A_2 z_1 - \Delta A_1 z_2}{z_1 z_2^* - z_2 z_1^*} z^*, \quad (\text{XXIII-47})$$

or $A = A_0 + Cz - C^* z^*, \quad (\text{XXIII-48})$

where
$$C = \frac{\Delta A_1 z_2^* - \Delta A_2 z_1^*}{z_1 z_2^* - z_2 z_1^*}. \quad (\text{XXIII-49})$$

Using Equation XXIII-47 it is an easy task to calculate

$$\frac{\partial A}{\partial z} = C = \frac{\Delta A_1 z_2^* - \Delta A_2 z_1^*}{z_1 z_2^* - z_2 z_1^*}. \quad (\text{XXIII-50})$$

Substituting this expression into Equation XXIII-41 and making the assumption that the reluctivity is constant, namely,

$$\gamma_2(|\mathbf{B}(\mathbf{r})|) \cong \gamma_2 = \text{constant} \quad (\text{XXIII-51})$$

and is not a function of $|\mathbf{B}(\mathbf{r})|$, the results are

$$\oint_C \gamma_2 \operatorname{Re} \left(2i \frac{\Delta A_1 z_2^* - \Delta A_2 z_1^*}{z_1 z_2^* - z_2 z_1^*} dl \right) = \mu_0 J_2 \frac{a_2}{3}. \quad (\text{XXIII-52})$$

Since the integrand is not a function of z it may be taken outside the integral sign. The result is

$$\gamma_2 \operatorname{Re} \left(2i \frac{\Delta A_1 z_2^* - \Delta A_2 z_1^*}{z_1 z_2^* - z_2 z_1^*} \right) \oint_C dl = \mu_0 J_2 \frac{a_2}{3}. \quad (\text{XXIII-53})$$

Before evaluating the line integral we recall that all six triangles will be used in the final equation for A_0 . The assumption is made that the effective $\mathbf{B}(\mathbf{r})$ field on the common side of any two adjacent triangles is the average of the $\mathbf{B}(\mathbf{r})$ fields in the two triangles.

Therefore the line integrals, in the opposite directions, along any of these common sides will cancel each other as illustrated in Figure XXIII-6. Triangles on the boundary will not have their path integrals canceled along the boundary. Figure XXIII-7 illustrates an advantage of this configuration: the sum over the entire problem area of Ampere's Law applied locally around each mesh point is equal to Ampere's Law applied around the boundary of the complete problem.

Returning to the geometry of Figure XXIII-4, we see that the only part of the integration path that can contribute to the final result is $C = (p_1, p_2, p_3)$, where the points p_1 and p_3 have coordinates given by the complex numbers

$$p_1 = \frac{z_1 + z_0}{2}, \quad (\text{XXIII-54})$$

and
$$p_3 = \frac{z_2 + z_0}{2}. \quad (\text{XXIII-55})$$

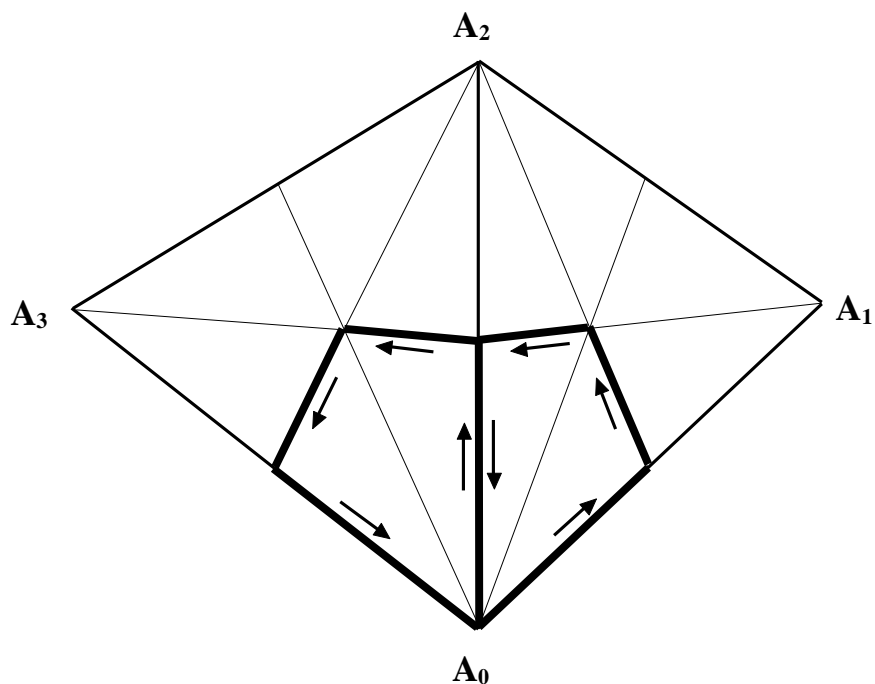


Figure XXIII-6. Integration paths in adjacent triangles.

It is assumed that the effective $B(r)$ on common sides of adjacent triangles are the same and, therefore, the line integrals along these common sides will cancel one another.

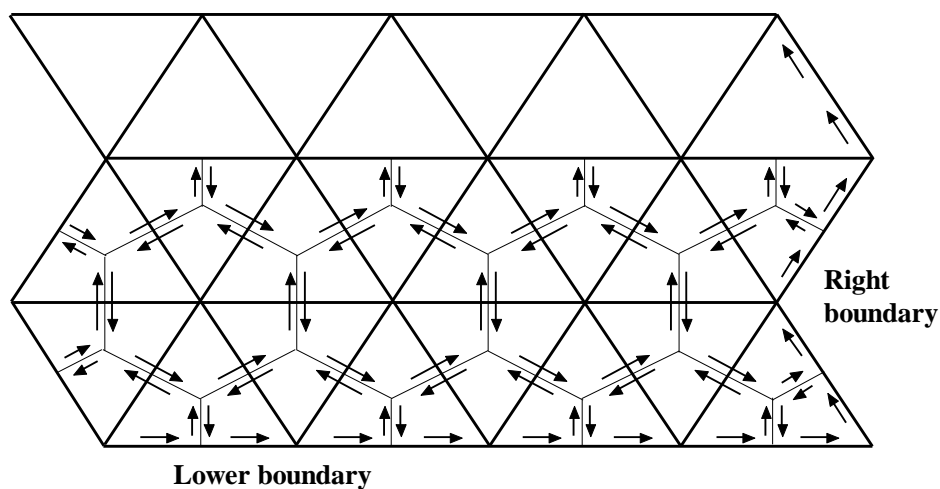


Figure XXIII-7. Cancellation of interior contours.

The sum of the contour integrals around each point adds up to a contour integral around the whole region because of cancellation of the interior contours.

The part of the contour integral that does not cancel is

$$\oint_C dl = \int_{p_1}^{p_2} dl + \int_{p_2}^{p_3} dl = (p_2 - p_1) + (p_3 - p_2) = p_3 - p_1$$

$$= \frac{z_2 + z_0}{2} - \frac{z_1 + z_0}{2} = \frac{z_2 - z_1}{2}. \quad (\text{XXIII-56})$$

Substituting this result into Equation XXIII-53 gives the equation

$$\gamma_2 \operatorname{Re} \left[i \frac{(\Delta A_1 z_2^* - \Delta A_2 z_1^*)(z_2 - z_1)}{z_1 z_2^* - z_2 z_1^*} \right] = \mu_0 J_2 \frac{a_2}{3}. \quad (\text{XXIII-57})$$

To obtain the real part of the quantity on the left-hand side of Equation XXIII-57, we express the positional variables z_i and z_i^* in terms of the angles β_0 , β_1 , and β_2 and the triangle-leg lengths d_0 , d_1 , and d_2 shown in Figure XXIII-4. Begin by evaluating the denominator, namely,

$$z_1 z_2^* - z_2 z_1^*. \quad (\text{XXIII-58})$$

The z terms can be expressed in exponential form as follows:

$$z_1 = d_2 e^{i\alpha_1}, \quad (\text{XXIII-59})$$

$$z_1^* = d_2 e^{-i\alpha_1}, \quad (\text{XXIII-60})$$

$$z_2 = d_1 e^{i(\alpha_1 + \beta_0)}, \quad (\text{XXIII-61})$$

$$z_2^* = d_1 e^{-i(\alpha_1 + \beta_0)}, \quad (\text{XXIII-62})$$

After substitution of these expressions the denominator becomes

$$\begin{aligned} z_1 z_2^* - z_2 z_1^* &= d_2 e^{i\alpha_1} d_1 e^{-i(\alpha_1 + \beta_0)} - d_1 e^{i(\alpha_1 + \beta_0)} d_2 e^{-i\alpha_1} \\ &= d_1 d_2 (e^{-i\beta_0} - e^{i\beta_0}) = -i 2 d_1 d_2 \sin \beta_0. \end{aligned} \quad (\text{XXIII-63})$$

Next, evaluate the numerator,

$$i (\Delta A_1 z_2^* - \Delta A_2 z_1^*) (z_2 - z_1), \quad (\text{XXIII-64})$$

using the relations

$$z_2 - z_1 = -d_0 \cos(\beta_1 - \alpha_1) + i d_0 \sin(\beta_1 - \alpha_1) = d_0 e^{i(\pi + \alpha_1 - \beta_1)}, \quad (\text{XXIII-65})$$

$$z_1^* (z_2 - z_1) = d_2 e^{-i\alpha_1} d_0 e^{i(\pi + \alpha_1 - \beta_1)} = -d_0 d_2 e^{-i\beta_1}, \quad (\text{XXIII-66})$$

$$z_2^*(z_2 - z_1) = d_1 e^{-i(\alpha_1 + \beta_0)} d_0 e^{i(\pi + \alpha_1 - \beta_1)} = -d_0 d_1 e^{i\beta_2}, \quad (\text{XXIII-67})$$

where in Equation XXIII-67 we have used the fact that $\beta_0 + \beta_1 + \beta_2 = \pi$. We find that the numerator can be written

$$i(\Delta A_1 z_2^* - \Delta A_2 z_1^*)(z_2 - z_1) = i(\Delta A_1 d_0 d_1 e^{i\beta_2} + \Delta A_2 d_0 d_2 e^{-i\beta_1}). \quad (\text{XXIII-68})$$

Having evaluated both the numerator and the denominator of Equation XXIII-57, we combine the results to obtain the following,

$$\begin{aligned} \operatorname{Re} \left[\frac{i(\Delta A_1 z_2^* - \Delta A_2 z_1^*)(z_2 - z_1)}{z_1 z_2^* - z_2 z_1^*} \right] &= \operatorname{Re} \left[\frac{i(\Delta A_1 d_0 d_1 e^{i\beta_2} + \Delta A_2 d_0 d_2 e^{-i\beta_1})}{-i 2 d_1 d_2 \sin \beta_0} \right] \\ &= \operatorname{Re} \left[\frac{\Delta A_1 d_0 d_1 (\cos \beta_2 + i \sin \beta_2) + \Delta A_2 d_0 d_2 (\cos \beta_1 - i \sin \beta_1)}{-2 d_1 d_2 \sin \beta_0} \right] \\ &= -\frac{\Delta A_1 d_0 d_1 \cos \beta_2}{2 d_1 d_2 \sin \beta_0} - \frac{\Delta A_2 d_0 d_2 \cos \beta_1}{2 d_1 d_2 \sin \beta_0} \\ &= -\frac{\Delta A_1 \cos \beta_2 \sin \beta_0}{2 \sin \beta_0 \sin \beta_2} - \frac{\Delta A_2 \cos \beta_1 \sin \beta_0}{2 \sin \beta_0 \sin \beta_1}, \end{aligned} \quad (\text{XXIII-69})$$

where we have used the fact that

$$\frac{d_0}{d_1} = \frac{\sin \beta_0}{\sin \beta_1}, \quad (\text{XXIII-70})$$

$$\text{and} \quad \frac{d_0}{d_2} = \frac{\sin \beta_0}{\sin \beta_2}. \quad (\text{XXIII-71})$$

The final expression is in terms of the cotangents of the interior angles and the vector potential at the vertices, namely,

$$\begin{aligned} \operatorname{Re} \left[\frac{i(\Delta A_1 z_2^* - \Delta A_2 z_1^*)(z_2 - z_1)}{z_1 z_2^* - z_2 z_1^*} \right] &= -\frac{1}{2} (\Delta A_1 \cot \beta_2 + \Delta A_2 \cot \beta_1) \\ &= -\frac{1}{2} [(A_1 - A_0) \cot \beta_2 + (A_2 - A_0) \cot \beta_1] \end{aligned}$$

$$= \frac{1}{2} \left[A_0 (\cot \beta_1 + \cot \beta_2) - A_1 \cot \beta_2 - A_2 \cot \beta_1 \right]. \quad (\text{XXIII-72})$$

Substituting this result into Equation XXIII-57 gives the relation

$$\frac{\gamma_2}{2} \left[A_0 (\cot \beta_1 + \cot \beta_2) - A_1 \cot \beta_2 - A_2 \cot \beta_1 \right] = \mu_0 J_2 \frac{a_2}{3}. \quad (\text{XXIII-73})$$

Change the angle representation from β 's to the θ 's shown in Figure XXIII-2. The result is

$$\frac{\gamma_2}{2} \left[A_0 (\cot \theta_3 + \cot \theta_4) - A_1 \cot \theta_4 - A_2 \cot \theta_3 \right] = \mu_0 J_2 \frac{a_2}{3}. \quad (\text{XXIII-74})$$

The complete line integral around the dodecagon is the sum of the partial paths over each of the triangles as shown in Figure XXIII-3, with the result

$$\begin{aligned} & \frac{\gamma_1}{2} \left[A_0 (\cot \theta_1 + \cot \theta_2) - A_1 \cot \theta_1 - A_6 \cot \theta_2 \right] \\ & + \frac{\gamma_2}{2} \left[A_0 (\cot \theta_3 + \cot \theta_4) - A_2 \cot \theta_3 - A_1 \cot \theta_4 \right] \\ & + \frac{\gamma_3}{2} \left[A_0 (\cot \theta_5 + \cot \theta_6) - A_3 \cot \theta_5 - A_2 \cot \theta_6 \right] \\ & + \frac{\gamma_4}{2} \left[A_0 (\cot \theta_7 + \cot \theta_8) - A_4 \cot \theta_7 - A_3 \cot \theta_8 \right] \\ & + \frac{\gamma_5}{2} \left[A_0 (\cot \theta_9 + \cot \theta_{10}) - A_5 \cot \theta_9 - A_4 \cot \theta_{10} \right] \\ & + \frac{\gamma_6}{2} \left[A_0 (\cot \theta_{11} + \cot \theta_{12}) - A_6 \cot \theta_{11} - A_5 \cot \theta_{12} \right] \\ & = \frac{\mu_0}{3} \sum_{i=1}^6 J_i a_i. \end{aligned} \quad (\text{XXIII-75})$$

We then solve equation XXIII-75 for A_0 and define the following “coupling” coefficients:

$$\begin{aligned} w_1 &= \frac{1}{2} (\gamma_1 \cot \theta_1 + \gamma_2 \cot \theta_4), \\ w_2 &= \frac{1}{2} (\gamma_2 \cot \theta_3 + \gamma_3 \cot \theta_6), \\ w_3 &= \frac{1}{2} (\gamma_3 \cot \theta_5 + \gamma_4 \cot \theta_8), \end{aligned}$$

$$w_4 = \frac{1}{2}(\gamma_4 \cot \theta_7 + \gamma_5 \cot \theta_{10}),$$

$$w_5 = \frac{1}{2}(\gamma_5 \cot \theta_9 + \gamma_6 \cot \theta_{12}),$$

$$w_6 = \frac{1}{2}(\gamma_6 \cot \theta_{11} + \gamma_1 \cot \theta_2).$$

The final result is

$$A_0 = \frac{\sum_{i=1}^6 A_i w_i + \frac{\mu_0}{3} \sum_{i=1}^6 J_i a_i}{\sum_{i=1}^6 w_i}. \quad (\text{XXIII-76})$$

C. Application of boundary conditions

Boundary conditions are divided into two classes:

- Dirichlet, where the value of the solution variable is specified on a boundary, and
- Neumann, where the value of the normal derivative of the solution variable is specified on a boundary.

Over any particular portion of the boundary only one type of boundary condition can be applied at a time. A Dirichlet boundary segment specifies A_z at each mesh point on the boundary. The default value is $A_z = 0$, but the user may input nonzero values, if necessary. For the Neumann boundary condition, the only allowed value for the normal derivative of A_z is zero, which can be written

$$\frac{\partial A_z}{\partial n} \hat{\mathbf{e}}_n = 0, \quad (\text{XXIII-77})$$

where $\hat{\mathbf{e}}_n$ is the unit vector normal to the boundary.

The Poisson Superfish codes maintain an array that indicates whether each point is on a Dirichlet boundary or not. However, similar information about Neumann boundaries is not stored in this way. The codes find Neumann boundaries by looking at the properties of triangles rather than mesh points. Figure XXIII-8 shows point 0 surrounded by its six nearest neighbors, numbered 1 through 6. Each point is associated with an upper and a lower triangle to its right. Points 0, 1, and 2 form the upper triangle of point 0. Points 0, 1, and 6 form its lower triangle. Figure XXIII-8 also shows the reluctivity γ_i for each triangle and a boundary line that separates the area into an interior region and an exterior region. Triangles in the exterior region have $\gamma = 0$ (in this example $\gamma_4 = \gamma_5 = \gamma_6 = 0$). Thus, if a point is not already marked as Dirichlet, the code looks for zero values of the reluctivity in the triangles to find Neumann boundaries.

The integration path around a point on a Neumann boundary is identical to the path shown in Figure XXIII-3 except that the path integral does not lie in triangles outside the boundary nor along the boundary itself. The contour path in Figure XXIII-8 is $C = (p_1, p_2, p_3, p_4, p_5, p_6, p_7)$. To show that the path integral along this Neumann boundary is zero, we first divide the closed path of integration into three parts as follows,

$$\oint_{C_1} \gamma(|\mathbf{B}(\mathbf{r})|) \mathbf{B}(\mathbf{r}) \cdot d\mathbf{l} + \oint_{C_2} \gamma(|\mathbf{B}(\mathbf{r})|) \mathbf{B}(\mathbf{r}) \cdot d\mathbf{l} + \oint_{C_3} \gamma(|\mathbf{B}(\mathbf{r})|) \mathbf{B}(\mathbf{r}) \cdot d\mathbf{l} = \mu_0 \int_S \mathbf{J}(\mathbf{r}) \cdot \hat{\mathbf{n}} da , \quad (\text{XXIII-78})$$

where C_1 is the path (p_0, p_1) , C_2 is the path $(p_1, p_2, p_3, p_4, p_5, p_6, p_7)$, and C_3 is the path (p_7, p_0) . Recalling that the vector functions $\mathbf{B}(\mathbf{r})$ and $\mathbf{A}(\mathbf{r})$ are two-dimensional, we write

$$\mathbf{B}(\mathbf{r}) = B_n \hat{\mathbf{e}}_n + B_t \hat{\mathbf{e}}_t . \quad (\text{XXIII-79})$$

and $\mathbf{A}(\mathbf{r}) = A_n \hat{\mathbf{e}}_n + A_t \hat{\mathbf{e}}_t + A_z \hat{\mathbf{e}}_z . \quad (\text{XXIII-80})$

and where $\hat{\mathbf{e}}_n$ is the unit vector normal to the boundary, and $\hat{\mathbf{e}}_t$ is the unit vector tangent to the boundary. Using Equation XXIII-4, namely,

$$\mathbf{B}(\mathbf{r}) = \nabla \times \mathbf{A}(\mathbf{r}) , \quad (\text{XXIII-81})$$

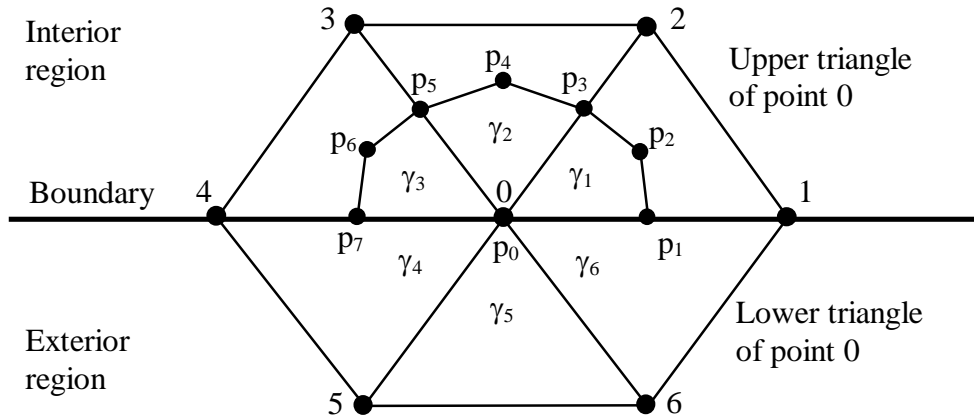


Figure XXIII-8. Path of contour integration on a Neumann boundary. Point 0 in the mesh is surrounded by six nearest neighbors, numbered 1 through 6. Associated with point 0 is an upper triangle and a lower triangle. Triangles outside the problem geometry will have $\gamma = 0$.

and expanding the curl in this reference system, one obtains the result

$$\mathbf{B}(\mathbf{r}) = \left(\frac{\partial A_z}{\partial t} - \frac{\partial A_t}{\partial z} \right) \hat{\mathbf{e}}_n + \left(\frac{\partial A_n}{\partial z} - \frac{\partial A_z}{\partial n} \right) \hat{\mathbf{e}}_t + \left(\frac{\partial A_t}{\partial n} - \frac{\partial A_n}{\partial t} \right) \hat{\mathbf{e}}_z. \quad (\text{XXIII-82})$$

The reasoning is still valid, as in Equation XXIII-7, that the components of $\mathbf{A}(\mathbf{r})$ in the two-dimensional plane are equal to zero, hence

$$A_n = A_t = 0. \quad (\text{XXIII-83})$$

The result of equating the coefficients of like unit vectors is

$$B_n = \frac{\partial A_z}{\partial t} \quad (\text{XXIII-84})$$

$$\text{and} \quad B_t = -\frac{\partial A_z}{\partial n}. \quad (\text{XXIII-85})$$

Since at a Neumann boundary

$$\frac{\partial A_z}{\partial n} = 0, \quad (\text{XXIII-86})$$

$$\text{then} \quad B_t = 0. \quad (\text{XXIII-87})$$

Hence, along the Neumann boundary

$$\mathbf{B}(\mathbf{r}) \cdot d\mathbf{l} = B_t dl = 0. \quad (\text{XXIII-88})$$

The path integrals along Neumann boundary segments will then be zero, that is

$$\oint_{C_1} \gamma(|\mathbf{B}(\mathbf{r})|) \mathbf{B}(\mathbf{r}) \cdot d\mathbf{l} = \oint_{C_3} \gamma(|\mathbf{B}(\mathbf{r})|) \mathbf{B}(\mathbf{r}) \cdot d\mathbf{l} = 0.$$

D. Calculation of fields

By definition in Poisson and Pandira, the magnetic induction $\mathbf{B}(\mathbf{r})$ is a two-dimensional vector function lying in the x-y plane:

$$\mathbf{B}(\mathbf{r}) = B_x \hat{\mathbf{e}}_x + B_y \hat{\mathbf{e}}_y, \quad (\text{XXIII-89})$$

and is equal to the curl of the vector potential $\mathbf{A}(\mathbf{r})$

$$\mathbf{B}(\mathbf{r}) = \nabla \times \mathbf{A}(\mathbf{r}) = \frac{\partial A_z}{\partial y} \hat{\mathbf{e}}_x - \frac{\partial A_z}{\partial x} \hat{\mathbf{e}}_y. \quad (\text{XXIII-90})$$

Equating the coefficients of like unit vectors of the above equation with those of the magnetic induction $\mathbf{B}(\mathbf{r})$ from Equation XXIII-89 give the required equations describing

the components of the magnetic induction over each triangle in terms of the only nonzero component of the vector potential A_z . Since the vector potential is linear over any triangle the magnetic induction $\mathbf{B}(\mathbf{r})$ will be constant over that triangle. The partial derivatives

$$B_x = \frac{\partial A_z}{\partial y}, \quad (\text{XXIII-91})$$

and
$$B_y = -\frac{\partial A_z}{\partial x}, \quad (\text{XXIII-92})$$

can then be evaluated analytically for any triangle in the mesh by using the positions (x , y) of the three vertices and their corresponding values for the vector potential component A_z at these points. The following equations are the results of evaluating Equation XXIII-37 and XXIII-38 using Equation. XXIII-47:

$$B_x = \frac{\partial A_z}{\partial y} = \frac{(A_2 - A_0)x_1 - (A_1 - A_0)x_2}{x_1y_2 - x_2y_1}, \quad (\text{XXIII-93})$$

$$B_y = -\frac{\partial A_z}{\partial x} = \frac{(A_2 - A_0)y_1 - (A_1 - A_0)y_2}{x_1y_2 - x_2y_1}. \quad (\text{XXIII-94})$$

For convenience, we take the origin for each triangle in the above equations at the point $(x_0, y_0) = (0, 0)$.

E. Computer algorithm using the SOR method

In the development of the algorithm that solves for the vector potential $\mathbf{A}(\mathbf{r})$ we assumed that the reluctivity γ is constant over a triangle and not a function of the magnetic induction $\mathbf{B}(\mathbf{r})$, namely

$$\gamma_i(|\mathbf{B}(\mathbf{r})|) \cong \gamma_i = \text{constant}. \quad (\text{XXIII-95})$$

This assumption was an expedient that we now deal with. The program uses an iterative procedure and solves for the vector potential one mesh point at a time, while also modifying the reluctivity of the surrounding six triangles. Referring to Figure XXIII-2, the procedure steps are as follows:

1. Given the current estimates for the vector potential (A_0 and its six surrounding mesh points A_1 through A_6) calculate new estimates of the reluctivity γ_1 through γ_6 associated with the six surrounding triangles. Use these values to compute new estimates of the coupling coefficients w_1^{new} through w_6^{new} . Rather than adopt these new values, use an “under relaxation” technique to avoid too large a change in one iteration:

$$w_i^{n+1} = qw_i^{\text{new}} + (1-q)w_i^n \quad (\text{XXIII-96})$$

where $0 < q < 1$.

2. Calculate a new estimate of the vector potential A_0 using a successive over-relaxation (SOR) technique,

$$A_0^{k+1} = A_0^k + \omega \left[\frac{\sum_{i=1}^3 A_i^k w_i^{n+1} + \sum_{i=4}^6 A_i^{k+1} w_i^{n+1} + \frac{\mu_0}{3} \sum_{i=1}^6 J_i a_i}{\sum_{i=1}^6 w_i^{n+1}} - A_0^k \right], \quad (\text{XXIII-97})$$

where $0 < \omega < 2$. The superscript index k in the above equation is a sweep counter of estimates and is not incremented until a convergence criterion for the vector potential is met.

3. Repeat steps 1 and 2 until a convergence criterion is met.

This procedure is followed for each mesh point as the program sequentially sweeps across points in the mesh.

F. Computer algorithm using the direct method

A direct method was developed for the program Pandira. It is direct in the sense that estimates of the vector potential for all the interior mesh points are calculated simultaneously. The procedure is still overall iterative in that the reluctivity of each triangle must be first estimated before the vector potentials can be calculated directly and then these two steps repeated again until a convergence criterion is met. The procedure is as follows:

1. Given the current estimates for the vector potential on all the mesh points calculate new estimates of the reluctivity γ_i associated with the all the interior triangles. Use these values to compute new estimates of the coupling coefficients w_i^{new} . As in the Poisson SOR method, use an “under relaxation” technique to avoid too large a change in one iteration:

$$w_i^{n+1} = q w_i^{\text{new}} + (1 - q) w_i^n \quad (\text{XXIII-98})$$

where $0 < q < 1$. [This comment about using the under-relaxation technique is from the 1987 manual. However, the procedure is not implemented in Pandira. The code simply replaces the reluctivity with the value computed from the permeability table.]

2. Calculate a new estimate of the vector potential A_i on all the mesh points by inverting a tridiagonal matrix. The number of equations is equal to the number of interior points to be solved. The following equation, applied at each mesh point, sets up the set of linear equations to be solved simultaneously:

$$A_0 = \frac{\sum_{i=1}^6 A_i w_i + \frac{\mu_0}{3} \sum_{i=1}^6 J_i a_i}{\sum_{i=1}^6 w_i} \quad (\text{XXIII-99})$$

3. Repeat steps 1 and 2 until a convergence criterion is met.